Application of a capillary electrophoresis-mass spectrometry metabolomics workflow in zebrafish larvae reveals new effects of cortisol

Mever, M. van; Mamani-Huanca, M.; Faught, L.E.; Lopez-Gonzalvez, A.; Hankemeier, T.; Barbas, C.; ... ; Ramautar, R.

Received: 21 August 2023 | Revised: 22 November 2023 | Accepted: 24 November 2023

DOI: 10.1002/elps.202300186

ELECTROPHORESIS

RESEARCH ARTICLE

Application of a capillary electrophoresis–mass spectrometry metabolomics workflow in zebrafish larvae reveals new effects of cortisol

Marlien van Mever[1] | **Maricruz Mamani-Huanca**[2] | **Erin Faught**[3] | **Ángeles López-Gonzálvez**[2] | **Thomas Hankemeier**[1] | **Coral Barbas**[2] | **Marcel J. M. Schaaf**[3] | **Rawi Ramautar**[1]

[1]Leiden Academic Centre for Drug Research (LACDR), Leiden University, Leiden, The Netherlands

[2]Centre for Metabolomics and Bioanalysis (CEMBIO), Department of Chemistry and Biochemistry, Facultad de Farmacia, Universidad San Pablo-CEU, CEU Universities, Urbanización Montepríncipe, Boadilla del Monte, Madrid, Spain

[3]Institute of Biology Leiden (IBL), Leiden University, Leiden, The Netherlands

Correspondence
Rawi Ramautar, Leiden Academic Centre for Drug Research (LACDR), Leiden University, 2333 CC Leiden, The Netherlands.
Email: r.ramautar@lacdr.leidenuniv.nl; rawi.ramautar@gmail.com

Color online: See the article online to view Figures 1–3 in color.

Funding information
Netherlands Organization of Scientific Research, Grant/Award Number: 723.016.003; International Doctoral School (CEINDO), Grant/Award Number: CEINDO-SANTANDER

Abstract

In contemporary biomedical research, the zebrafish (*Danio rerio*) is increasingly considered a model system, as zebrafish embryos and larvae can (potentially) fill the gap between cultured cells and mammalian animal models, because they can be obtained in large numbers, are small and can easily be manipulated genetically. Given that capillary electrophoresis–mass spectrometry (CE–MS) is a useful analytical separation technique for the analysis of polar ionogenic metabolites in biomass-limited samples, the aim of this study was to develop and assess a CE–MS-based analytical workflow for the profiling of (endogenous) metabolites in extracts from individual zebrafish larvae and pools of small numbers of larvae. The developed CE–MS workflow was used to profile metabolites in extracts from pools of 1, 2, 4, 8, 12, 16, 20, and 40 zebrafish larvae. For six selected endogenous metabolites, a linear response ($R^2 > 0.98$) for peak areas was obtained in extracts from these pools. The repeatability was satisfactory, with inter-day relative standard deviation values for peak area of 9.4%–17.7% for biological replicates ($n = 3$ over 3 days). Furthermore, the method allowed the analysis of over 70 endogenous metabolites in a pool of 12 zebrafish larvae, and 29 endogenous metabolites in an extract from only 1 zebrafish larva. Finally, we applied the optimized CE–MS workflow to identify potential novel targets of the mineralocorticoid receptor in mediating the effects of cortisol.

KEYWORDS
capillary electrophoresis–mass spectrometry, glucocorticoid receptor, metabolomics, mineralocorticoid receptor, zebrafish larvae

Abbreviations: CE–MS, capillary electrophoresis–mass spectrometry; GR, glucocorticoid receptor; GSH, glutathione; GSSG, glutathione disulfide; IS, internal standard; MR, mineralocorticoid receptor; MRKO, MR-knockout; MS-222, tricaine mesylate; QC, Quality control; ROS, reactive oxygen species; RSD, relative standard deviation; RPLC, reversed-phase liquid chromatography; SIL, stable-isotope-labeled.

Marlien van Mever, Maricruz Mamani-Huanca, and Erin Faught Equally contributed as first authors

1 | INTRODUCTION

Zebrafish (*Danio rerio*) are increasingly used as a model system in biomedical research, mainly because of their genetic and cellular homology with mammals [1]. Other advantages of this species include their rapid development (zebrafish larvae have functioning organs and a complex behavioral repertoire a few days post-fertilization [dpf]) and high production of offspring (100–200 eggs), allowing for high throughput studies [2, 3]. Furthermore, zebrafish are an increasingly use model in predictive animal model studies of human physiology.

To study metabolism in zebrafish larvae, a number of analytical techniques have been considered, with chromatography-based techniques coupled to mass spectrometry (MS) being the most popular, including RPLC–MS [4], hydrophilic interaction chromatography–MS [5], and gas chromatography–MS [6], this often requires pooling of 100 of larvae. Additionally, direct infusion MS [2] and nuclear magnetic resonance spectroscopy [7] have been used. Capillary electrophoresis–MS (CE–MS) could be considered an attractive technique for zebrafish larvae analysis, mainly due to its microscale character, low sample consumption and complementary separation mechanism toward chromatographic techniques. The potential of CE–MS was already demonstrated for metabolic profiling of zebrafish larvae by our group [8], using CE–MS with a flow-through micro vial interface for the analysis of an extract from a single zebrafish larva (48 h post fertilization). However, only a few metabolites could be detected with that approach and the coupling of CE to MS via this interface was quite complicated; moreover, analytical performance metrics, including of this method for metabolomics studies, have not been demonstrated so far. In comparison, the use of a conventional co-axial sheath-liquid interface for coupling CE to MS has proven to be robust and reproducible for metabolomics studies, as shown in a recent Metabo-ring study [9]. Shanmuganathan and co-workers have developed a robust sheath-liquid CE–MS-based workflow for metabolic profiling of more than 1000 serum samples from a multi-ethnic cohort of pregnant women with an acceptable precision [10]. Harada and co-workers used sheath-liquid CE–MS for the comprehensive profiling of charged and polar metabolites in more than 8000 human plasma samples from the Tsuruoka Metabolomics Cohort Study over a 52-month period [11]. In our group we have recently demonstrated that sheath-liquid CE–MS is well-suited for the efficient and sensitive profiling of polar ionogenic metabolites in various volume-restricted biological samples, demonstrating the value of this method for probing metabolic changes in biomass-restricted model systems [12, 13].

In this study, a CE–MS-based workflow has been developed for the profiling of polar ionogenic metabolites in extracts from zebrafish larvae in order to study the effects of cortisol, a hormone that is secreted upon stress. Within the last decade, zebrafish have proven to be a very effective model for stress research, in particular for studies on the effects of cortisol [14, 15]. These effects are mediated by two nuclear receptors, the glucocorticoid receptor (GR) and the mineralocorticoid receptor (MR). These receptors have different affinities for cortisol, with GR being activated at high cortisol levels and MR being already activated at basal cortisol levels. Although the role of cortisol-GR signaling during stress is well characterized [16], the role of MR on mediating the effects of cortisol is less known [17, 18]. The exact biological response to a stressor and the associated increase in cortisol levels is highly individualized, as it depends on factors such as genetic background, biological age, and personality [19]. In this context, metabolomics, that is, the analysis of (endogenous) small molecules within a biological system, could be considered a valuable approach to gain a deeper understanding of the molecular responses occurring after exposure to cortisol. For this purpose, wild-type (WT) and ubiquitous MR-knockout (MRKO) zebrafish larvae were used and exposed to exogenous cortisol treatment. So far, it has hardly been investigated what the specific role of MR is during stress on metabolite levels, and which mechanisms might be important in this association.

2 | MATERIALS AND METHODS

2.1 | Chemicals and reagents

All chemicals used were of analytical grade or higher purity. Acetic acid (99%), methanol, and propan-2-ol were acquired from Biosolve. Ammonium hydroxide (28%) was purchased from Acros Organics. Sodium hydroxide and hydrochloric acid were of 98% and 37% purity, respectively, and were purchased from Merck and Thermo Fisher Scientific. Amino acids standards were from Sigma-Aldrich. ^{13}C and/or ^{15}N stable-isotope labeled (SIL) internal standards were purchased from Cambridge Isotope Laboratories. A Milli-Q Advantage A10 water purification system (Merck) was used to obtain pure water. Ascorbic acid was from Sigma-Aldrich.

Ascorbic acid was used as an antioxidant. A stock solution of 1 mg/mL was prepared in water, and a working solution with a final concentration of 125 μM was prepared by dilution with water. A working solution of ascorbic acid was prepared daily. Background electrolyte (BGE) solution was prepared by diluting acetic acid in water (10% v/v). As sheath-liquid, a mixture of water and propan-2-ol (50:50,

v/v), containing 0.03% (v/v) acetic acid was used. Prior to first use, the sheath liquid was degassed for 10 min.

2.2 | Sample solutions

SIL metabolite standards (1 mg/mL) were dissolved in a Milli-Q water. SIL metabolite mixtures of eight compounds (Table S1) were prepared in water as 100 µM stock solutions, aliquoted and stored at −20°C. Migration time (MT) markers procaine, paracetamol, and methionine sulfone were prepared in water as 100 µM mixed solutions, aliquoted and stored at −20°C. The final concentration of MT markers was 50 µM.

2.3 | Zebrafish larvae maintenance and cortisol treatment

Adult zebrafish (*D. rerio*; AB/Tupfel long fin strain) were maintained in compliance with the directives of the local animal welfare committee of Leiden University. Specifically adults were housed on a recirculating system (Fleuren & Nooijen) on a 14:10 light:dark cycle. Water was maintained at 28.5°C, pH 7.4, 300 µS conductivity, and 10% of the water was exchanged daily. Animals were fed twice daily with Gemma micro 500 diet (Skretting) in the morning and live *Artemia* (Great Salt Lake Brine Shrimp Cooperative) in the afternoon.

A zebrafish WT strain and zebrafish mutants lacking a functional MR (designated nr3c2$^{inrl1/inrl1}$, hereafter called MRKO). WT and MRKO zebrafish larvae were maintained at 28.5°C in 20 × 100 mm^2 plates with 1 × E3 medium (5 mM NaCl, 0.17 mM KCl, 0.33 mM $CaCl_2$, 0.33 mM $MgSO_4$ + 0.1 ppm methylene blue antifungal agent), with daily water changes until 3 dpf, according to guidelines of the zebrafish Model Organism Database (zfin.org). At 3 dpf, larvae were transferred to 6-well plates (20 fish/well) and treated with either cortisol (5 µg/mL) or a vehicle control (0.05% ethanol). The larvae were then raised to 5 dpf, and all treatments were refreshed daily. Larvae were euthanized with an overdose of 0.4 mg/L tricaine mesylate (MS-222) purchased from Sigma-Aldrich. A pool of 1, 2, 4, 8, 12, 16, 20, and 40 larvae were collected, and each pool was considered a sample.

2.4 | Experimental design

To study the role of MR in the metabolic response to cortisol in zebrafish larvae, a workflow using CE–MS has been developed and the following experimental design has been designed (see Figure 1). First, homogenization and metabolite extraction were optimized, then the number of larvae per sample was set. Four groups have been used to survey the involvement of MR. For this purpose, WT zebrafish larvae and MRKO zebrafish larvae were used, both groups were stimulated with 5 µg/mL cortisol (F) (WT-F and MRKO-F) and by 0.05% ethanol as a control-vehicle (V) (WT-V and MRKO-V).

2.5 | Zebrafish larvae homogenization and metabolite extraction

To determine the most optimal sample preparation protocol, three homogenization strategies were compared for zebrafish larval samples and were carried out using homogenization based on probe homogenization (DIAX 900; Heidolph) as strategy 1, homogenization using a bullet blender using ~10 stainless steel beads (BBX24; Next Advance) as strategy 2, and homogenization based on tip sonication (Q125, Qsonica) as strategy 3. The conditions for each of the strategies are shown in Table 1, and each was repeated three times. For each strategy, pools of eight zebrafish larvae were used in 50 µL of methanol in a 1.5 mL Eppendorf tube and three main steps were followed. First, extraction solvent was added according to each strategy (see Table 1). The second step was the homogenization of the samples. Finally, the homogenate was centrifuged (16 100 × g, 5 min, 4°C), and 450 µL (strategy 1) or 90 µL (strategies 2 and 3) supernatant was pipetted into a 0.5 mL Eppendorf vial. The samples were evaporated in a Speed-Vac Vacuum concentrator (Thermo Savant SC210A), and reconstituted in 20 µL BGE prior to injection.

To determine the recovery of each strategy, SIL internal standards were spiked in the zebrafish larvae samples before homogenization and after sample preparation. Recovery was calculated based on the following formula:

$$\%\text{recovery} = \frac{\text{area IS spiked before}}{\text{area IS spiked after}} \times 100\%.$$

2.6 | CE–MS-based metabolic profiling of zebrafish larvae extracts

Metabolic profiling was carried out with the 7100 CE system from Agilent Technologies which was coupled to a 6230 time of flight-MS instrument from Agilent using a co-axial sheath-liquid electrospray ionization (ESI) interface equipped with a triple-tube sprayer, also from Agilent. Sheath-liquid was delivered at a final flow rate of 3 µL/min by an Agilent 1260 Infinity Isocratic Pump (Agilent Technologies) with a flow splitter that splits the sheath liquid in the ratio 1:100. Fused-silica capillaries with an internal

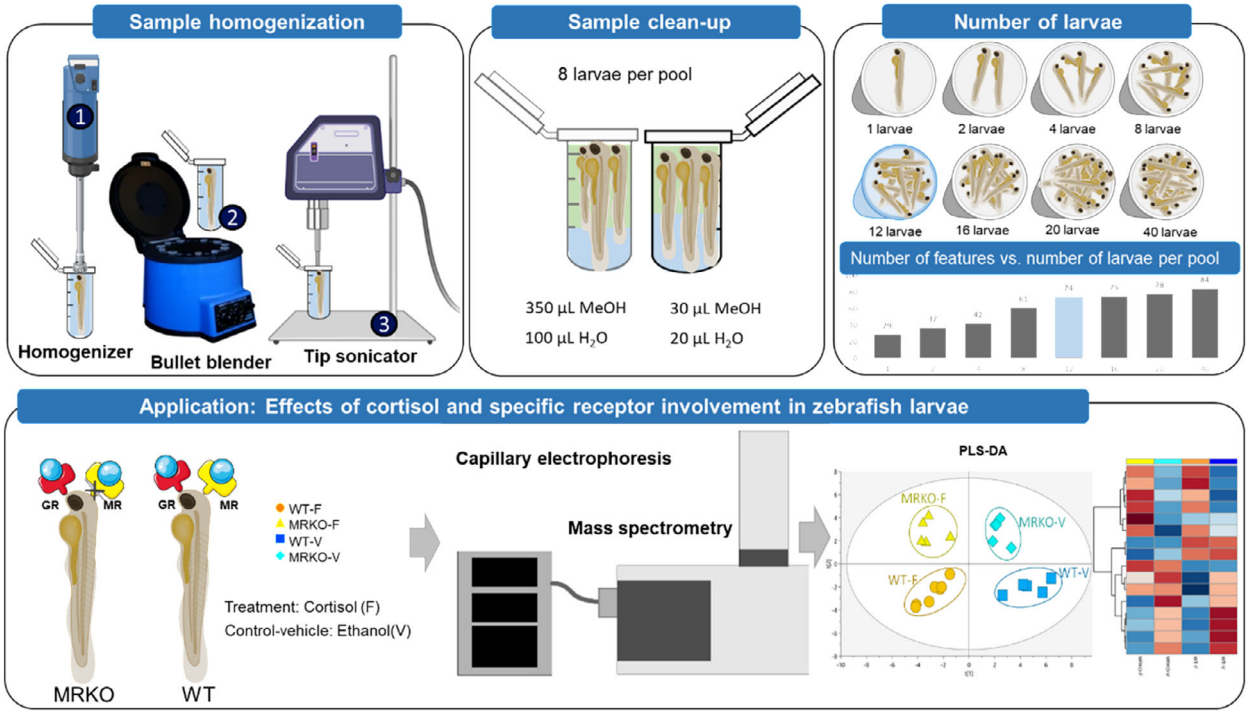

FIGURE 1 Workflow developed to study the effects of cortisol and involvement of specific receptors in zebrafish larvae using capillary electrophoresis coupled to mass spectrometry. *Source*: Figure created with Biorender.com.

TABLE 1 Conditions used for each strategy to determine the best method of metabolite extraction from zebrafish larvae.

Strategy	Extraction solvent	Sample homogenization
1	400 µL cold methanol 80 µL cold water 10 µL ascorbic acid (125 µM) 10 µL water with IS (100 µM)	Homogenizer (1000 × *g*, 30 s)
2	80 µL cold methanol 10 µL ascorbic acid (125 µM) 10 µL water with IS (100 µM)	Bullet blender (500 × *g*, 5 min)
3	80 µL cold methanol 10 µL ascorbic acid (125 µM) 10 µL water with IS (100 µM)	Tip sonication (1 × 3 s pulse, 30% amplitude)

Abbreviation: IS, Internal standard.

diameter of 50 µm were purchased from BGB Analytik, and cut to a total length of 90 cm. New capillaries were conditioned by subsequently rinsing, at 5 bar for 1 min, with methanol, water, sodium hydroxide 1 M, water, hydrochloric acid 1 M, water and BGE. Injections were performed hydrodynamically for 54 s at 50 mbar (35.3 nL), and injected volumes were calculated with Zeecalc v1.0b (https://epgl.unige.ch/labs/fanal/zeecalc). For metabolite separation, a voltage of 30 kV was applied. The current observed during the experiment under these conditions was 12.9 µA. MS experiments were acquired in positive mode between 50 and 1000 *m/z* with an acquisition rate of 1.5 spectra/s. The nebulizer gas was set to 0 psi, and the sheath gas flow rate and temperature were set at 11 L/min and 100°C, respectively and both were nitrogen. The ESI capillary voltage was set to 5500 V. Fragmentor and skimmer voltages were set at 100 and 50 V, respectively. In order to obtain information about fragments, in-source fragmentation was used, applying 200 V at the fragmentor. MassHunter version B.06.00 (Agilent) was used for data acquisition, instrument control and data treatment. From the sheath-liquid, propan-2-ol ($C_3H_8OH^+$) and its

clusters ($[(C_3H_8O)_2+H]^+$ and $([(C_3H_8O)_3+H]^+$) with corresponding *m/z* values of 61.06479, 121.12231 and 181.17982, respectively, were used as lock masses.

2.7 | Data processing

Peak extraction was performed using MassHunter Quantitative Analysis (B.10.00, Agilent Technologies) with a mass error of 20 ppm and peak integrations were visually inspected to ensure correct integration. The response function of the measured peak area for 6 endogenous metabolites (aspartic acid, lysine, asparagine, glutamic acid, glutamine, and 2 aminobutyric acid) of which SIL internal standards were available for each was examined using 3 biological replicates for at least 8 different numbers of zebrafish larvae pools (from 40 larvae down to 1 larva). Methionine sulfone, procaine, and paracetamol were used as internal standards and included with the SIL mixture, all with a concentration of 50 µM. Repeatability (expressed as percentage relative standard deviation [%RSD]) for peak area was determined by analyzing SIL standards spiked into a zebrafish sample ($n = 3$). The last experiment has been repeated on three consecutive days to determine interday precision.

The data deconvolution process for the untargeted metabolomics was processed using MassHunter Profinder (B.10.00, Agilent Technologies), to obtain a data matrix in an appropriate format. Two consecutive algorithms were used in the software to perform the deconvolution. The first, performs the molecular features extraction, reduces the data by removing non-specified information. The second algorithm, Find by Ion was used for targeted feature extraction and to obtain a better accuracy of the data. Finally, abundance of the molecule, mass accuracy and MT for each feature in all samples were obtained as matrix data [20]. Data quality was ensured by excluding background noise and unrelated ions, molecular features present in 50% of the quality control (QC) injections with a RSD less than 30%, and present in 75% of the study samples, were maintained. Missing values were estimated using the *k*-nearest neighbours algorithm.

Subsequently, the matrix was normalized by the total useful signal, and then an unsupervised principal component analysis (PCA-X) model was generated in order to observe the trend of the QCs, detect outliers, and observe natural clustering trends.

2.8 | Statistical analysis

Multivariate data analysis was used to investigate the differences between the four groups. Supervised models such as the partial least square discriminant analysis (PLS-DA) and orthogonal PLS–DA (OPLS–DA) were performed to discriminate the variation between groups. The quality of the models was evaluated by explained variance (R^2) evaluating the model by maximizing the variance given by the variables and predicted variance (Q^2) evaluating the predictive ability of the model. These parameters were provided by SIMCA-P (Version 17, Umetrics, Sartorius Stedim Biotech) software. Finally, the percentage change was calculated by comparing cases with controls.

2.9 | Metabolite identification

Compounds were tentatively annotated based on their exact mass, isotopic distribution, and adduct formation using the CEU Mass mediator search tool [21]. Furthermore, to enhance confidence in metabolite identification, relative MTs, effective mobility values (μ_{eff}) [9, 22], and in-source fragments were compared with respect to standards analysed in a previous experiment [23].

3 | RESULTS AND DISCUSSION

3.1 | CE–MS analysis of zebrafish larvae

In metabolomics studies, typically, the efficient homogenization of tissues and extraction of metabolites from tissue homogenates are the steps that are most time-consuming and error-prone. Therefore, as a first step, the homogenization and metabolite extraction were evaluated for zebrafish larvae samples. For metabolite extraction, a single-phase extraction method based on protein precipitation with methanol was selected due to its effective capability to precipitate proteins [24, 25], speed and simplicity [26].

For the sample preparation, three different homogenization strategies were tested, that is, homogenization based on standard homogenization (strategy 1), homogenization using a bullet blender (strategy 2), and homogenization based on tip sonication (strategy 3). All three strategies were applied to small pools of zebrafish larvae (8 larvae per pool) of 5 dpf. SIL standards (50 µM) were spiked into the zebrafish larvae sample before and after sample preparation to determine the recovery and repeatability of the different strategies. After complete homogenization, homogenates were collected. After metabolite extraction, the metabolite content of the homogenates was analyzed using CE–MS, and the recoveries of SIL standards were calculated. As shown in Table S2, satisfactory recoveries were observed for all three homogenization strategies: between 84% and 98% for strategy 1, between 88% and 107% for

strategy 2, and between 100% and 104% for strategy 3. Moreover, the repeatability of peak areas of SIL standards was determined for SIL standards spiked at the beginning of the workflow for biological replicates as the %RSD and was between 6.3% and 17.3% for strategy 1, between 4.5% and 15.0% for strategy 2 and between 3.1% and 8.4% for strategy 3.

Another important aspect during tissue homogenization is metabolite stability, as degradation could occur due to time duration, (high) temperatures and the applied frequency. As is expected that catecholamines such as epinephrine and dopamine play an important role in mediating the stress response in zebrafish larvae [27], precautions were taken by adding an antioxidant at the beginning of the workflow in order to stabilize metabolites throughout the sample preparation. As antioxidant, ascorbic acid (12.5 μM) was selected due to its compatibility with MS detection [28]. Additionally, at pH 2.2, ascorbic acid will have no net charge, causing it to migrate with the electroosmotic flow and thereby not disturbing the detection of cationic metabolites of interest. To evaluate the metabolite stability during sample preparation, two catecholamines epinephrine and dopamine, which are well-known metabolites that are prone to degradation, were included in the SIL standard mixture. As is shown in Table S2, good recoveries for epinephrine and dopamine were observed for all homogenization strategies, with 96% and 98% for strategy 1%, 88%, and 96% for strategy 2 and 101% and 101% for strategy 3, which indicates there is no significant loss during sample preparation.

Furthermore, when selecting an appropriate sample preparation strategy, the time duration per sample is an important factor. Due to the size of the homogenizer tip for strategy 1, a minimal total volume of 500 μL needs to be present in the Eppendorf vial in order to perform proper homogenization, whereas in the case of the bullet blender and tip homogenizer, 100 μL of total volume showed to be sufficient. After extraction, homogenization and centrifugation, either 450 μL (strategy 1) or 90 μL (strategies 2 and 3) of supernatant was transferred into another Eppendorf vial and dried in a Speedvac. Because the increased volume of strategy 1, the time for evaporation was more than tripled (2+ h instead of 30 min). Additionally, because zebrafish larvae at 5 dpf encompass approximately 300 nL volume, it would be most beneficial to have as little dilution as possible during sample preparation. When comparing the time duration per sample for strategies 2 and 3, homogenization by the bullet blender takes 5 min per 24 samples (~13 s per sample), whereas tip sonication takes 3 s per sample. Taking into account the recovery and repeatability as well as the duration of the sample preparation strategy, strategy 3 (homogenization by tip sonication) was selected for further experiments.

The analytical performance of the CE–MS workflow was further evaluated for pools containing a small number of zebrafish larvae (8 fish per pool). Precision of the CE–MS workflow for profiling of endogenous metabolites in zebrafish larvae was assessed based on the repeated analyses of zebrafish samples spiked with glutamine-^{13}C as SIL internal standard (50 μM). Intraday RSD values ($n = 3$) were obtained with the analyte areas corrected with the glutamine ^{13}C area of the SIL and are shown in Table S3. Results for all endogenous analytes for biological replicates were between 0.9% and 20.3%, whereas interday RSDs ($n = 3$ over 3 days) were below 28.2% for 20% endogenous metabolites detected.

Subsequently, the response function of endogenous metabolites in decreasing numbers of zebrafish larvae per pool were investigated using SIL standards. Zebrafish pools of 40, 20, 16, 12, 8, 4, 2, and 1 zebrafish were spiked with SIL epinephrine-D_3, gamma-aminobutyric acid-D_6, glutamine-^{13}C, glutamic acid-^{13}C,^{15}N, asparagine-^{13}C,^{15}N, lysine-^{13}C and aspartic acid-^{13}C,^{15}N (50 μM), and calibration curves for endogenous metabolites corrected by their corresponding SIL analog were prepared (in case the endogenous metabolites were detected). A linear response (and with $R^2 > 0.98$) for selected metabolites was obtained (Figure S1A). Thereafter, it was investigated how many features could be extracted from the data resulting from the different zebrafish pools. As can be seen in Figure S1B, 84 features were found in a pool of 40 zebrafish larvae, whereas only 29 features could be extracted from a single zebrafish larva. For this study, the zebrafish pools containing 12 larvae were selected for further experiments, as a lower amount of larvae showed to result in more efficient metabolite homogenization when employing low solvent volumes during sample preparation. Furthermore, for our application it was not necessary to show inter-individual differences between the fish, therefore making it unnecessary to further scale down the amount of fish per pool.

3.2 | Application of CE–MS to a zebrafish stress model

With the developed CE–MS workflow the aim was to study the role of polar ionogenic metabolites in zebrafish under a stress scenario and thus to potentially reveal the role of MR in mediating the effects of cortisol. After sample analysis, data processing was performed. The signals were then filtered for presence in blanks, in clusters and in QC samples with a %RSD less than 30%. Then the signals belonging to adducts and fragments were removed. The final data set was reduced to 61 compounds (Table S4). The analytical performance of CE–MS was evaluated using the

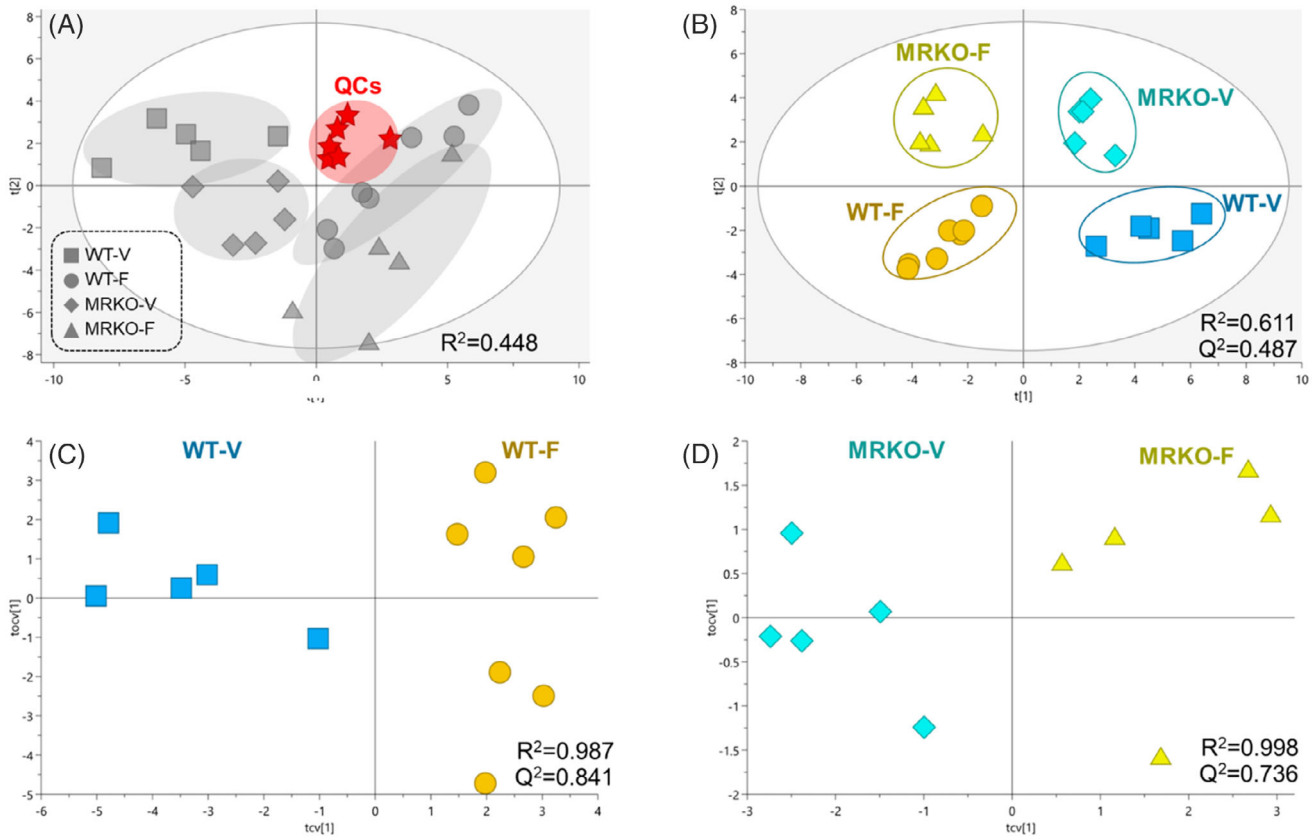

FIGURE 2 (A) Principal component analysis (PCA-X) score plot with an explained variance $R^2 = 0.448$, quality control (QC, red starts), (B) partial least square–discriminant analysis (PLS–DA) model, (C) CV-orthogonal PLS (OPLS)-DA model for wild-type (WT)-F ($n = 7$) versus WT-V ($n = 5$) comparison, and (D) CV-OPLS-DA model for mineralocorticoid receptor-knockout (MRKO)-F ($n = 5$) versus MRKO-V ($n = 5$) comparison.

unsupervised PCA-X ($R^2 = 0.448$), resulting in a clustering of QC samples (QC's) distributed along the working list, showing high sensitivity and reproducibility throughout the analysis, indicating adequate data quality performance (Figure 2A).

Additionally, a supervised clustering PLS–DA model was constructed to obtain a better separation. The PLS–DA analysis score plot showed a clear separation between the four groups of cortisol-stimulated zebrafish larvae and controls. The PLS–DA model had an R^2 value of 0.611 and Q^2 value of 0.487 (Figure 2B). After this evaluation, OPLS–DA analysis was performed to compare two groups at a time. First, we compared the group of Wild type zebrafish larvae stimulated with cortisol (WT-F) versus the group of Wild type zebrafish larvae stimulated with ethanol as control (WT-V), the model presented an R^2 value of 0.987 and Q^2 value of 0.841 (Figure 2C). Then, the groups of MRKO zebrafish larvae stimulated with cortisol (MRKO-F) versus the group groups of MRKO zebrafish larvae stimulated with ethanol (MRKO-V) as a control were compared, the model presented an R^2 value of 0.998 and Q^2 value of 0.736 (Figure 2D).

To select the metabolites responsible for the clustering and separation of the groups from the OPLS–DA models, Jack-Knife confidence intervals were calculated, and variables importance in projection >1 and p (corr) > |0.5| were considered. In addition, for all OPLS–DA models, the validated cross-sectional scores plots were shown, which revealed that 99% of the samples were correctly classified in their corresponding group. The results for the WT-F to WT-V and MRKO-F to MRKO-V comparisons of multivariate statistics are shown in Table 2.

The WT-F group was compared to WT-V, as a result 12 metabolites appeared to be modulated in response to stress. Increases in sarcosine, alanine, cytosine, *N*-acetylspermidine, and cytidine levels were observed. In contrast, levels of serine, asparagine, ornithine, aspartic acid, cystathione, gutation disulfide, and Asp–Lys were decreased (Table 2). On the other hand, MRKO-F larvae were compared with MRKO-V larvae. As a result, 11 metabolites were modulated. Increases in sarcosine, alanine, cytosine, acetylcholine, *N*-acetylspermidine, and cytidine levels were observed. However, decreased levels of serine, ornithine, aspartic acid, glutathione (GSH)

TABLE 2 Differentially identified metabolite contents in the comparison of cortisol-stimulated zebrafish larval groups and control groups.

			WT-F versus WT-V				MRKO-F versus MRKO-V			
Name	**Mass (Da)**	**RSD (%) QC**	***p* (Corr)**	**VIP**	**JK**	**change (%)**	***p* (Corr)**	**VIP**	**JK**	**change (%)**
Sarcosine	89.0475	8.0	0.9	1.6	Yes	58.8	0.9	1.8	Yes	47.5
Alanine	89.0476	2.4	0.9	1.4	Yes	23.2	0.8	1.7	Yes	12.8
Serine	105.0420	4.3	−1	1.6	Yes	−37.6	−0.8	1.7	Yes	−23.4
Cytosine	111.0427	27.6	0.7	1.3	Yes	83.9	0.5	1.1	–	47.2
Asparagine	132.0527	3.8	−0.8	1.4	Yes	−23.2	−0.6	1.1	–	−9.5
Ornithine	132.0890	7.2	−0.9	1.6	Yes	−66.6	−0.9	1.7	Yes	−49
Aspartic acid	133.0368	4.6	−0.5	1.0	–	−15.5	−0.7	1.6	Yes	−37.7
Acetylcholine	145.1091	6.0	NS	<1	–	NS	0.6	1.3	Yes	36.1
N^1-acetylspermidine	187.1670	10.2	0.7	1.2	–	50.2	0.6	1.4	Yes	56.5
Cystathionine	222.0692	9.1	−0.6	1.2	Yes	−26.8	NS	<1	–	NS
Cytidine	243.0845	12.3	0.7	1.3	Yes	47.6	0.6	1.2	–	45
Aspartyllysine[a]	261.1314	20.5	−0.7	1.2	Yes	−49.9	−0.6	1.3	–	−40.6
Glutathione disulfide	612.1478	27.4	−0.8	1.4	Yes	−54.6	NS	<1	–	NS

Abbreviations: JK, confidence intervals derived from jack-knife; MRKO, mineralocorticoid receptor-knockout; MT, migration time; NS, No significative; RMT, relative migration; VIP, variables importance in projection; WT, wild-type.

[a]Contains multiple annotation options.

disulfide, and Asp-Lys were observed (Table 2). Those metabolites that are altered in WT but not in MRKO were observed to highlight MR-dependent metabolites.

The effects of cortisol on MR expression, we compared MRKO versus WT zebrafish larvae, both stimulated with cortisol. Upon comparison, we observed increases in the levels of sarcosine, serine, cystathionine and Glu–Pro. However, decreases in the levels of *N*-acetyl-glucosaminate and an unknown mass-neutral compound 324.1486 were observed (Table S5 and Figure S2). In addition, the effects of ethanol stimulation on zebrafish larvae were also evaluated. After comparison of MRKO with WT zebrafish larvae, increases in the levels of sarcosine, serine, 4-guadininobutanal, histidine, and Glu–Pro were observed, whereas the levels of threonine, ornithine, *N*-acetyl-glucosaminate, and an unknown compound (mass 324.1486) decreased (Table S5 and Figure S2).

3.3 | Discussion and interpretation of the main findings

Cortisol is the main stress hormone in humans and zebrafish, responsible for a suite of metabolic changes post-stress designed to restore homeostasis. Even though the role of cortisol-GR signaling is well characterized, little is known regarding the role of MR in cortisol-induced metabolic changes. Here we used CE–MS, to not only identify novel pathways impacted by cortisol signaling, but also optimized this technique for use in single larvae. Taken together, we present here an untargeted study based on CE–MS to determine the role of polar metabolites in mediating the GR and MR response to stress.

We first evaluated the involvement of GR and MR in the metabolic profile of larvae post cortisol treatment, metabolites that were found to be commonly modulated following cortisol stimulation in both WT and MRKO zebrafish larvae compared to their respective controls were alanine, sarcosine, serine, cytosine, asparagine, ornithine, aspartic acid, *N*-acetyl-spermidine, cytidine, and Asp–Lys. These metabolites are likely regulated by cortisol-GR signaling as GR is the primary receptor for cortisol in MRKO larvae. However, MR signaling may still be involved because often the cortisol-induced change in metabolite level in WT larvae could not be fully recapitulated in MRKO larvae. For example, alanine levels increase 23% in WT larvae but only 12% in MRKO larvae. A similar trend was also observed in the case of sarcosine, cytosine, *N*-acetylspermidine, and cytidine, as well as slight decreases in the levels of serine, asparagine, ornithine, Asp–Lys, and aspartic acid (Table 2). These findings support the essential functions described for GR in energy homeostasis, stress response, and inflammation, while revealing that the cooperation between GR and MR may also be important for metabolic homeostasis [29].

Stress and the attendant rise in cortisol has been associated with increased reactive oxygen species (ROS) and nitrogen species leading to oxidative and nitrosative stress [30]. Ornithine is a substrate for putrescine production and complements polyamine metabolism, which may explain the decrease in ornithine levels during both GR activation and GR and MR cooperation in response to stress.

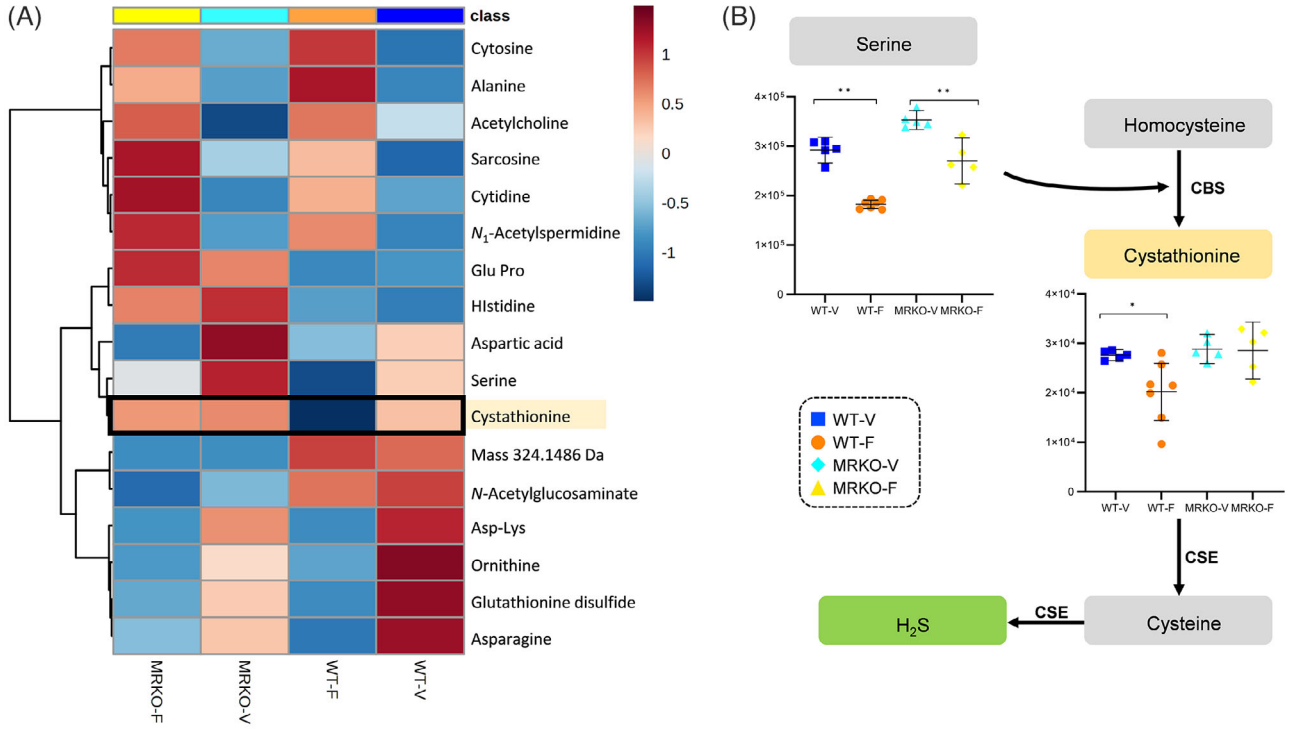

FIGURE 3 (A) The heat map shows the mean abundance of the 17 metabolites found to be modulated in the metabolomic analysis of cortisol-stimulated wild-type (WT) or mineralocorticoid receptor-knockout (MRKO) versus their respective controls. Metrics used for the analysis were the Euclidean distance measure and Ward's clustering algorithm using MetaboAnalyst 5.0 software. (B) Biogenesis of H_2S by CSE or CBS.

Polyamines such as putrescine and spermidine are essential for decreasing ROS damage in animals [31] and for protecting from stress, allowing the flow of K1 current, controlling brain glutamate receptors implicated in learning and memory [32]. On other hand, we found higher increased levels of *N*-acetylspermidine in cortisol treated larvae, when GR is activated, however, we did not find alterations in putrescine and spermidine levels. Spermidine is a substrate of spermidine/spermine *Nź*-acetyltransferas, which is responsible for promoting acetylation at N^1 in the presence of acetyl-CoA resulting in N^1-acetylspermidine which in turn is converted to putrescine. These results suggested that GR promotes the acetylation of spermidine by altering the regulatory metabolism of polyamines [33]. In addition, ornithine is a substrate for proline production and contributes to the formation of glutamate. Glutamate is the main excitatory neurotransmitter in the central nervous system, and its regulation is important for maintaining the balance of the glutamate cycle. It has been reported that glutamatergic dysfunction causes neuropsychiatric conditions such as stress, anxiety and depression [34].

Another metabolite that was modulated by the effects of cortisol was an *N*-methylated derivative of glycine. Sarcosine is produced from glycine via glycine *N*-methyltransferase which utilizes a methyl group from *S*-adenosylmethionine [35]. Sarcosine has been described to be an inhibitor of glycine transporter-1, increasing the levels of glycine, an inhibitor of rapid neurotransmission. Sarcosine is also responsible for enhancing the function of the *N*-methyl-D-aspartate receptor [35]. Previous studies have shown that sarcosine has a neuroprotective effect as it is effective in reducing oxidative stress [36]. These findings could justify the increase in sarcosine levels in response to cortisol during GR and MR activation and their cooperation with each other.

Moreover, decreases in asparagine and aspartic acid levels have been observed in response to cortisol stimulation in both GR activation and GR and MR cooperation. Aspartic acid is converted to asparagine through asparagine synthetase using glutamine in response to cellular stress [37]. Glutamate and aspartate are both excitatory neurotransmitters, with aspartate as the most abundant in the central nervous system. Additionally, aspartate is converted to alanine via aspartate 4-decarboxylase [38, 39].

On the other hand, acetylcholine levels were found to be increased under cortisol conditions in MRKO larvae compared to MRKO-V, whereas in WT-F compared to WT-V acetylcholine was not significant. This could suggest that MR may restrict GR-dependent increase in acetylcholine

levels. The dominant negative effect of MR on GR transcriptional activation has been observed both in vitro and in vivo. This finding suggests that the balance between GR and MR is essential to maintain acetylcholine levels.

As previously mentioned, cortisol exposure causes increased oxidative stress resulting from the generation of ROS contributing to cell death. GSH acts as an antioxidant defense and is responsible for the direct scavenging of ROS. During ROS scavenging, GSH interacts with radicals such as superoxide radical anion, nitric oxide, or hydroxyl radical. On the other hand, GSH is an electron donor for the reduction of peroxides in the glutathione peroxidase reaction with the final oxidation product being glutathione disulfide (GSSG). However, GSH is regenerated from GSSG through the reaction catalyzed by GSH reductase [40]. In our study, decreased levels of GSSG were found in response to cortisol stimulation in WT fish larvae, whereas in MRKO the percentage change was not significant. This suggests that MR may be a key player in activation of the antioxidant protection system.

In addition, cystathionine regulation was observed to be MR-dependent only. Cystathionine is produced by cystathionine beta synthase an enzyme that catalyses the first step of the transsulfuration pathway, leading to the production of cystathionine from serine and homocysteine. It has been described that under stress cystathionine levels are decreased consistent with what was observed in cortisol treated WT larvae in this study. Here we show that this decrease is likely due to MR as the effect of cortisol on cystathionine was abolished when MR was absent. Cystathionine can then be converted to cysteine and by extension H_2S by the enzyme cystathionine gamma lyase to produce H_2S from cysteine and homocysteine (Figure 3) [41]. H_2S is associated with many physiological processes, such as inflammation, neuromodulation and apoptosis, and abnormal levels are associated with Alzheimer's diseases, liver cirrhosis and diabetes [42]. The data here suggests that MR may be a key regulator of enzymes involved in cystathionine production and subsequently impact key physiological processes.

Taken together, in this study we have optimized a CE–MS workflow, which allowed us to establish metabolic profiles in biomass-limited samples. As a proof of concept, we examined the metabolic impact of cortisol treatment in zebrafish larvae, and identified novel targets of MR.

4 | CONCLUDING REMARKS

In this work, a CE–MS-based analytical workflow has been developed for the profiling of polar ionogenic metabolites in extracts from zebrafish larvae with acceptable performance metrics. The workflow has been used successfully used for the profiling of metabolites in extracts from WT and zebrafish with a ubiquitous MRKO, providing insights into the role of MR and GR in mediating the effects of cortisol.

Through the present study, besides the ability of GR to modulate metabolism independently of MR, we observed the cooperation of both receptors in maintaining the balance of the metabolome, and that part of this profile is regulated by MR. Indeed, differential regulation of cystathionine by MR has been identified, even though this metabolite is known to be modulated during stress. Taken together, this technique has the potential to identify novel pathways and mechanisms of action in zebrafish larvae.

ACKNOWLEDGMENTS

The authors of this work acknowledge the financial support of the Vidi grant scheme of the Netherlands Organization of Scientific Research (NWO Vidi 723.016.003). M.M-H would like to acknowledge the CEU- International Doctoral School (CEINDO) grant and the CEINDO-SANTANDER research mobility grant.

Open access funding provided by VSNU.

CONFLICT OF INTEREST STATEMENT

The authors have declared no conflict of interest.

DATA AVAILABILITY STATEMENT

The data that support the findings of this study are available from the corresponding author upon reasonable request.

ORCID

Marlien van Mever https://orcid.org/0000-0002-4951-7815
Ángeles López-Gonzálvez https://orcid.org/0000-0002-6363-7135
Coral Barbas https://orcid.org/0000-0003-4722-491X
Rawi Ramautar https://orcid.org/0000-0002-1673-4848

REFERENCES

1. Schlegel A, Gut P. Metabolic insights from zebrafish genetics, physiology, and chemical biology. Cell Mol Life Sci. 2015;72:2249–60.
2. Raterink RJ, Kloet F, Li J, Wattel N, Schaaf M, Spaink H, et al. Rapid metabolic screening of early zebrafish embryogenesis based on direct infusion-nano ESI-FTMS. Metabolomics. 2013;9:864–73.
3. Santoro MM. Zebrafish as a model to explore cell metabolism. Trends Endocrinol Metab. 2014;25:546–54.
4. Ribbenstedt A, Posselt M, Brunius C, Benskin JP. In-plate toxicometabolomics of single zebrafish embryos. Mol Omics. 2020;16:185–94.
5. Tufi S, Leonards P, Lamoree M, de Boer J, Legler J, Legradi J. Changes in neurotransmitter profiles during early zebrafish (*Danio rerio*) development and after pesticide exposure. Environ Sci Technol. 2016;50:3222–30.

6. Dhillon SS, Torell F, Donten M, Lundstedt-Enkel K, Bennett K, Rannar S, et al. Metabolic profiling of zebrafish embryo development from blastula period to early larval stages. PLoS One. 2019;14:e0213661.
7. Mushtaq MY, Marçal RM, Champagne DL, van der Kooy F, Verpoorte R, Choi YH. Effect of acute stresses on zebra fish (*Danio rerio*) metabolome measured by NMR-based metabolomics. Planta Med. 2014;80:1227–33.
8. Lindenburg PW, Ramautar R, Jayo RG, Chen DDY, Hankemeier T. Capillary electrophoresis–mass spectrometry using a flow-through microvial interface for cationic metabolome analysis. Electrophoresis. 2014;35:1308–14.
9. Drouin N, van Mever M, Zhang W, Tobolkina E, Ferre S, Servais AC, et al. Capillary electrophoresis–mass spectrometry at trial by metabo-ring: effective electrophoretic mobility for reproducible and robust compound annotation. Anal Chem. 2020;92:14103–12.
10. Shanmuganathan M, Kroezen Z, Gill B, Azab S, de Souza RJ, Teo KK, et al. The maternal serum metabolome by multisegment injection-capillary electrophoresis–mass spectrometry: a high-throughput platform and standardized data workflow for large-scale epidemiological studies. Nat Protoc. 2021;16:1966–94.
11. Harada S, Hirayama A, Chan Q, Kurihara A, Fukai K, Lida M, et al. Reliability of plasma polar metabolite concentrations in a large-scale cohort study using capillary electrophoresis–mass spectrometry. PLoS ONE. 2018;13:e0191230.
12. van Mever M, Segers K, Drouin N, Guled F, Vander Heyden Y, Van Eeckhaut A, et al. Direct profiling of endogenous metabolites in rat brain microdialysis samples by capillary electrophoresis–mass spectrometry with on-line preconcentration. Microchem J. 2020;156:104949.
13. Segers K, Zhang W, Aourz N, Bongaerts J, Declerck S, Mangelings D, et al. CE-MS metabolic profiling of volume-restricted plasma samples from an acute mouse model for epileptic seizures to discover potentially involved metabolomic features. Talanta. 2020;217:121107.
14. de Abreu MS, Demin KA, Giacomini ACVV, Amstislavskaya TG, Strekalova T, Maslov GO, et al. Understanding how stress responses and stress-related behaviors have evolved in zebrafish and mammals. Neurobiol Stress. 2021;15:100405.
15. Sireeni J, Bakker N, Jaikumar G, Obdam D, Slabbekoorn H, Tudorache C, et al. Profound effects of glucocorticoid resistance on anxiety-related behavior in zebrafish adults but not in larvae. Gen Comp Endocrinol. 2020;292:113461.
16. Finsterwald C, Alberini CM. Stress and glucocorticoid receptor-dependent mechanisms in long-term memory: from adaptive responses to psychopathologies. Neurobiol Learn Mem. 2014;112:17–29.
17. Joëls M, de Kloet ER. 30 Years of the mineralocorticoid receptor: the brain mineralocorticoid receptor: a saga in three episodes. J Endocrinol. 2017;234:T49–T66.
18. Faught E, Vijayan MM. The mineralocorticoid receptor is essential for stress axis regulation in zebrafish larvae. Sci Rep. 2018;8:18081.
19. Mifsud KR, Reul JMHM. Mineralocorticoid and glucocorticoid receptor-mediated control of genomic responses to stress in the brain. Stress. 2018;21:389–402.
20. Ciborowski M, Adamska E, Rusak M, Godzien J, Wilk J, Citko A, et al. CE–MS-based serum fingerprinting to track evolution of type 2 diabetes mellitus. Electrophoresis. 2015;36:2286–93.
21. Gil-de-la-Fuente A, Godzien J, Saugar S, Garcia-Carmona R, Badran H, Wishart DS, et al. CEU mass mediator 3.0: a metabolite annotation tool. J Proteome Res. 2019;18:797–802.
22. Mamani-Huanca M, de la Fuente AG, Otero A, Gradillas A, Godzien J, Barbas C, et al. Enhancing confidence of metabolite annotation in capillary electrophoresis–mass spectrometry untargeted metabolomics with relative migration time and in-source fragmentation. J Chromatogr A. 2021;1635:461758.
23. Mamani-Huanca M, Gradillas A, López-Gonzálvez Á, Barbas C. In-source fragmentation for the identification of compounds by CE-ESI-TOF in human plasma. L-proline as case study. Methods Mol Biol. 2022;2531:185–202.
24. Polson C, Sarkar P, Incledon B, Raguvaran V, Grant R. Optimization of protein precipitation based upon effectiveness of protein removal and ionization effect in liquid chromatography–tandem mass spectrometry. J Chromatogr B Biomed Appl. 2003;785:263–75.
25. Blanchard J. Evaluation of the relative efficacy of various techniques for deproteinizing plasma samples prior to high-performance liquid chromatographic analysis. J Chromatogr B Biomed Appl. 1981;226:455–60.
26. Da Silva KM, Iturrospe E, Bars C, Knapen D, Van Cruchten S, Covaci A, et al. Mass spectrometry-based zebrafish toxicometabolomics: a review of analytical and data quality challenges. Metabolites. 2021;11:635.
27. Kvetnansky R, Sabban EL, Palkovits M. Catecholaminergic systems in stress: structural and molecular genetic approaches. Physiol Rev. 2009;89:535–606.
28. Van Schoors J, Viaene J, Van Wanseele Y, Smolders I, Dejaegher B, Vander Heyden Y, et al. An improved microbore UHPLC method with electrochemical detection for the simultaneous determination of low monoamine levels in *in vivo* brain microdialysis samples. J Pharm Biomed Anal. 2016;127:136–46.
29. Gomez-Sanchez E, Gomez-Sanchez CE. The multifaceted mineralocorticoid receptor. Compr Physiol. 2014;4:965–94.
30. Flaherty RL, Owen M, Fagan-Murphy A, Intabli H, Healy D, Patel A, et al. Glucocorticoids induce production of reactive oxygen species/reactive nitrogen species and DNA damage through an iNOS mediated pathway in breast cancer. Breast Cancer Res. 2017;19:35.
31. Casero RA, Pegg AE. Polyamine catabolism and disease. Biochem J. 2009;421:323–38.
32. Pegg AE. The function of spermine. IUBMB Life. 2014;66:8–18.
33. Lentile R, Luca G, Giorgio RM, Macaione S. Glucocorticoid regulation of spermidine acetylation in the rat brain. J Neurochem. 1988;51:677–82.
34. Rosdy MS, Rofiee MS, Samsulrizal N, Salleh MZ, Teh LK. Understanding the effects of *Moringa oleifera* in chronic unpredictable stressed zebrafish using metabolomics analysis. J Ethnopharmacol. 2021;278:114290.
35. Yoon JK, Kim DH, Koo JS. Implications of differences in expression of sarcosine metabolism-related proteins according to the molecular subtype of breast cancer. J Transl Med. 2014;12:149.
36. Tanas A, Tozlu ÖÖ, Gezmiş T, Hacimüftüoğlu A, Abd El-Aty AM, Ceylan O, et al. *In vitro* and *in vivo* neuroprotective effects of sarcosine. BioMed Res Int. 2022;2022:5467498.

37. Balasubramanian MN, Butterworth EA, Kilberg MS. Asparagine synthetase: regulation by cell stress and involvement in tumor biology. Am J Physiol Endocrinol Metab. 2013;304:789–99.
38. Kurauchi I, Yamane H, Tsuneyoshi Y, Denbow DM, Furuse M. Central L-alanine reduces energy expenditure with a hypnotic effect under an acute stressful condition in neonatal chicks. Amino Acids. 2009;36:131–35.
39. Shigemi K, Tanaka K, Hayamizu K, Denbow DM, Furuse M. L-serine decreases taurine concentration in the extracellular fluid of brain slices. Neurosci Med. 2011; 2:268–74.
40. Pannala VR, Bazil JN, Camara AKS, Dash RK. A biophysically based mathematical model for the catalytic mechanism of glutathione reductase. Free Radic Biol Med. 2013;65:1385–97.
41. Pal VK, Bandyopadhyay P, Singh A. Hydrogen sulfide in physiology and pathogenesis of bacteria and viruses. IUBMB Life. 2018;70:393–410.
42. Kimura Y, Goto YI, Kimura H. Hydrogen sulfide increases glutathione production and suppresses oxidative stress in mitochondria. Antioxid Redox Signal. 2010;12:1–13.

SUPPORTING INFORMATION

Additional supporting information can be found online in the Supporting Information section at the end of this article.

How to cite this article: van Mever M, Mamani-Huanca M, Faught E, López-Gonzálvez Á, Hankemeier T, Barbas C, et al. Application of a capillary electrophoresis–mass spectrometry metabolomics workflow in zebrafish larvae reveals new effects of cortisol. Electrophoresis. 2024;45:380–91.
https://doi.org/10.1002/elps.202300186